

# Temporal Pulse Compression Beyond the Fourier Transform Limit

Alex M. H. Wong and George V. Eleftheriades, *Fellow, IEEE*

**Abstract**—It is a generally known that the Fourier transform limit forbids a function and its Fourier transform to both be sharply localized. Thus, this limit sets a lower bound to the degree to which a band-limited pulse can be temporally compressed. However, seemingly counterintuitive waveforms have been theoretically discovered, which, across finite time intervals, vary faster than their highest frequency components. While these so-called superoscillatory waveforms are very difficult to synthesize due to their high amplitude sidebands and high sensitivity, they open up the possibility toward arbitrarily compressing a temporal pulse, without hindrances from bandwidth limitations. In this paper, we report the design and realization of a class of superoscillatory electromagnetic waveforms for which the sideband amplitudes, and hence, the sensitivity can be regulated. We adapt Schelkunoff's method for superdirectivity to design such temporally compressed superoscillatory pulses, which we ultimately realize in an experiment, achieving pulse compression 47% improved beyond the Fourier transform limit.

**Index Terms**—Fourier transform limit, pulse compression, pulse shaping, superdirectivity.

## I. INTRODUCTION

THE availability of narrow pulses is essential to scientific experiments and instrumentation across the electromagnetic spectrum—from microwave to optical frequencies and beyond. However, regardless of the frequency of interest, the mathematical uncertainty principle provides a lower bound to the bandwidth-temporal width product of the electromagnetic waveform [1], thus forbidding a pulse to have a temporal width narrower than about the reciprocal of its bandwidth. This limitation is more often known in the engineering community as the Fourier transform limit. Since a waveform becomes transform limited when all its frequency components are phase aligned, most works on narrow pulse generation follow this simple general strategy: obtain the widest possible spectrum, then align the phase of all spectral components to generate a transform-limited pulse. Various practical difficulties have been resolved towards transform-limited pulse generation for both microwave and optical regimes. Arbitrary pulse shaping has been demonstrated at the microwave range using microstrip-based filters that shape the amplitude and phase spectra of microwave impulses [2],

[3]; few cycle, near transform-limited optical pulses have also been demonstrated in various laboratory environments [4]–[6]. It would appear as though the only way to obtain narrower pulses is to further extend the waveform bandwidth—which is a subject of intense research, particularly in the optical regime.

There is, however, another route to bypass the Fourier transform limit to obtain short temporal pulses. Properties of the Fourier transform do not forbid the existence of so-called superoscillatory functions, which, over finite intervals, oscillate much faster than their high-frequency band limit [7]–[9]. Through this effect, one can obtain a widened effective bandwidth within some finite temporal interval, and thereby construct waveforms with narrow peaks and rapid varying features without actually possessing a wide bandwidth. Hence, superoscillations enable one to construct an ultrashort temporal pulse beyond that allowed in the Fourier transform limit. (See the Appendix for further details.)

Though first introduced for quantum mechanical systems [7]–[9], superoscillations are theorized to occur in a wide range of waveforms including time-domain waveforms. It has even been suggested that an entire musical symphony can be encoded within a signal of 1-Hz bandwidth [8]. However, superoscillatory waveforms have proven difficult to realize. While several methods have been suggested for designing superoscillatory waveforms [9]–[11], temporal superoscillations have yet to be realized in experiment, likely due to two major reasons. Firstly, it is commonly thought that superoscillatory waveforms contain uncontrolled sidebands outside the region of superoscillatory behavior, whose amplitude could be orders of magnitude higher than the peak amplitude within the region of superoscillatory behavior. Secondly, it is also perceived that the construction of superoscillatory waveforms involves a very high degree of sensitivity. These perceptions make superoscillatory pulse compression seem both challenging and impractical. In the following, we introduce a superoscillatory pulse design method that allows one to design a waveform's superoscillatory region, but at the same time also control the sideband amplitude, and thus arrive at practical superoscillatory waveforms with reasonable waveform sensitivity. This ultimately allows us to demonstrate practical temporal pulse compression beyond the Fourier transform limit.

## II. THEORY AND FORMULATION

### A. Schelkunoff Approach to Designing Temporal Superoscillatory Waveforms

In a previous study, we concluded that superdirectivity is actually a superoscillation phenomenon in the spatial-frequency

Manuscript received October 08, 2010; revised June 13, 2011; accepted June 20, 2011. Date of publication August 04, 2011; date of current version September 14, 2011. This work was supported in part by the Natural Science and Engineering Research Council of Canada (NSERC).

The authors are with the Department of Electrical and Computer Engineering, University of Toronto, Toronto, ON, Canada M5S 3G4 (e-mail: alex.wong@utoronto.ca; gelefth@waves.utoronto.ca).

Color versions of one or more of the figures in this paper are available online at <http://ieeexplore.ieee.org>.

Digital Object Identifier 10.1109/TMTT.2011.2160961

and space domains [12]. With this in mind, in the following we adapt antenna design techniques to design temporal superoscillatory waveforms. First we define the spectrum of our waveform as a sum of sinusoidal harmonics—or, equivalently, as a sum of equi-spaced delta functions

$$\tilde{V}(\omega) = \sum_{n=0}^{N-1} a_n \delta(\omega - \omega_0 - n\Delta\omega) \quad (1)$$

where  $\omega$  is the angular frequency,  $\omega_0$  represents the location of the lowest (most negative) frequency delta function,  $\Delta\omega$  is the frequency spacing between adjacent tones, and  $a_n$  is the weight for the  $n$ th delta function. The temporal waveform is then written as

$$V(t) = \frac{1}{2\pi} \int_{-\infty}^{\infty} \tilde{V}(\omega) e^{i\omega t} d\omega = \frac{e^{i\omega_0 t}}{2\pi} \sum_{n=0}^{N-1} a_n z^n \quad (2)$$

where  $z = e^{i\Delta\omega t}$ . We note that (1) is analogous to current excitations on equi-spaced elements of an array, while (2) is analogous to the corresponding array factor polynomial. At this point, one can draw upon established works on discrete filter design [13] to place the  $N - 1$  zeros in the polynomial, and thereby design a waveform that is periodic in  $t$  with the Bloch period  $T = 2\pi/\omega$ .

Schelkunoff, in his pioneering work on superdirective antennas [14], showed that for antenna arrays with elements placed less than half-wavelength apart, the antenna's visible region is mapped onto the  $z$ -plane as an arc along the unit circle, but subtends an angle less than  $2\pi$  from the origin. Hence, if one close packs all available zeros along this arc, one can generate rapid variations, and thereby obtain narrow beamwidths in the outgoing antenna pattern. Drawing on the similarity between (1) and (2) and relevant equations in antenna array design, we extend Schelkunoff's theory into the time domain, and conclude the following: by close-packing zeros into a design time-interval  $T_d$  within its Bloch period  $T = 2\pi/\omega$ , one can design a waveform that contains desired superoscillatory features within  $T_d$  while sacrificing some degrees of control in the interval outside  $T_d$ .

We demonstrate the above formulation through two design examples: rapid superoscillatory oscillations and superoscillatory pulse compression.

### B. Design of Rapid Superoscillations

We first consider the fastest nonsuperoscillatory oscillation that can be generated with a given bandwidth. This oscillation will be a sinusoid of the highest constituent frequency, achieved when

$$a_n = \begin{cases} 1, & n = 0 \text{ or } N - 1 \\ 0, & \text{otherwise.} \end{cases} \quad (3)$$

Substituting (3) into (2) yields

$$V(t) = \frac{e^{i\omega_0 t}}{2\pi} (z^{N-1} + 1) = \frac{e^{i\omega_0 t}}{2\pi} \prod_{n=1}^{N-1} (z - z_n) \quad (4)$$

where  $z_n = \exp\left(i\left(-\frac{\pi}{N-1} + n\Delta\phi\right)\right)$  and  $\Delta\phi = \frac{2\pi}{N-1}$ . Thus,  $N - 1$  zeros for this sinusoid are equi-spaced across the unit  $z$ -circle with angular spacing  $\Delta\phi$ .

To obtain superoscillations at a frequency  $R$  times this highest frequency ( $R > 1$ ), the zeros within the design region  $T_d$  must appear  $R$  times as frequent

$$\Delta\phi' = \frac{\Delta\phi}{R} = \frac{2\pi}{(N-1)R}. \quad (5)$$

Close-packing zeros in such a manner within the design interval will lead to the desired rapid oscillation. Obviously one must ensure that the number of available zeros is sufficient for the proposed operations before one can generate the rapid oscillation for the desired time interval. On the other hand, if there are zeros left over from this shaping procedure, they can be used to shape the region outside  $T_d$ , to control, for example, the amplitude of the sideband.

### C. Design of a Superoscillatory Sharp Pulse

We borrow from relevant works on superdirective antennas [15], [16] to design a Chebyshev superoscillatory pulse, which is compressed beyond the Fourier-transform limit. To determine zero locations for the construction of such a Chebyshev temporal waveform, we simplify the notation in (2) for an even spectrum as follows:

$$V(t) = \sum_{n=-\lfloor N/2 \rfloor}^{\lfloor N/2 \rfloor} b_n z^n = b_0 + 2 \sum_{n=1}^{\lfloor N/2 \rfloor} b_n \cos(n\Delta\omega t) \quad (6)$$

where  $z = e^{i\Delta\omega t}$ .  $b_n$  in (6) differ from  $a_n$  in (2) by a factor of  $2\pi$ , a constant phase offset, and a change in index. We now introduce  $u = \text{Re}\{z\} = \cos(\Delta\omega t)$  with which we rewrite (6) as

$$\begin{aligned} V(t) &= b_0 + 2 \sum_{n=1}^{\lfloor N/2 \rfloor} b_n \cos(n \cos^{-1} u) \\ &= b_0 + 2 \sum_{n=1}^{\lfloor N/2 \rfloor} b_n T_n(u) \end{aligned} \quad (7)$$

where  $T_n(\cdot)$  is the  $n$ th-order Chebyshev polynomial of the first kind, defined as [17]

$$T_n(u) = \begin{cases} \cos(n \cos^{-1} u), & \text{for } |u| \leq 1 \\ \cosh(n \cosh^{-1} u), & \text{for } |u| > 1. \end{cases} \quad (8)$$

The property of relevance of the Chebyshev polynomial is that its amplitude remains bounded below unity for the interval  $|u| \leq 1$ , but rises rapidly for  $|u| > 1$ . In our design, we wish to locate zeros within a design interval  $|t| \leq T_d/2$ , and obtain the sharpest pulse while keeping sidelobes within the design interval at a level  $1/p$  that of the peak pulse amplitude. We achieve that by the mapping

$$u \rightarrow \nu = c_1 u + c_2 \quad (9)$$

subject to the boundary conditions

$$u = \cos\left(\Delta\omega\frac{T_d}{2}\right) \rightarrow \nu = -1$$

and

$$u = \cos(0) \rightarrow \nu' \text{ such that } T_{\lfloor N/2 \rfloor}(\nu') = p. \quad (10)$$

With this mapping, solving the decomposition relation

$$T_{\lfloor N/2 \rfloor}(\nu) = b_0 + 2 \sum_{n=1}^{\lfloor N/2 \rfloor} b_n T_n(u) \quad (11)$$

generates the spectral weights  $b_n$  up to a multiplicative constant. Finally, factoring (6) converts  $b_n$  into a set of zero locations needed to synthesize a Chebyshev waveform. For  $T_d < T$ , and the ratio  $1/p$  comparable to the first sidelobe amplitude for a normalized sinc pulse, the Chebyshev pulse designed in this manner is superoscillatory, and the pulsewidth surpasses the Fourier transform limit.

We end this section by comparing our temporal superoscillatory sharp pulse with a superdirective antenna beam. First and foremost, both waveforms achieve unconventional ‘‘sharpness’’ in that the temporal superoscillatory pulse breaks the Fourier transform limit, while the superdirective antenna beam breaks the angular diffraction limit, or the diffraction limit for directivity [18]. However, the manifestation of sidebands differs for these two effects. Sidebands remain part of the temporal waveform in our proposed approach to temporal superoscillatory pulse shaping, but they are pushed into the evanescent region, and rendered invisible in the case of antenna superdirectivity. This difference arises because the far-field mapping process in antenna theory does not find an analog in temporal superoscillation theory. The reader is referred to [12] for additional information. The sidebands—visible or invisible—contribute to power and sensitivity considerations in designing temporal superoscillatory pulses and superdirective beams. For superoscillations, it has been proven that energy in sidebands varies polynomially with the superoscillatory region’s apparent spectral width, and exponentially with its duration [19]. For superdirective antennas, it has been found that the antenna’s  $Q$  (ratio between stored and radiated power, or equivalently, the energy ratio between evanescent and propagating-wave components) increases approximately exponentially with directivity [20]. Thus, in both cases, there exist strong tradeoffs between resolution and power residing in the sidebands, the latter of which also effects the sensitivity of the waveform. As noted in Section I, sensitivity has been an impediment towards practical implementations of time-domain superoscillatory waveforms. Nonetheless, in the following, we will show that with our design methodology, one can appreciably compress a pulse from the Fourier transform limit, and still attain a reasonable tolerance on sensitivity.

### III. REALIZATION OF SUPEROSCILLATORY WAVEFORMS

#### A. Experimental Overview

In our proceeding experiments, we design and synthesize two superoscillatory signals  $V(t)$  as time-varying voltage

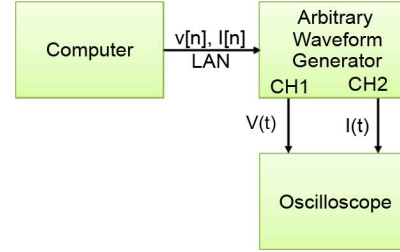


Fig. 1. Schematic of the experimental setup.  $V[n]$  and  $I[n]$  denote the discrete voltage and impulse sequences inputted to the AWG, while  $V(t)$  and  $I(t)$  denote the continuous time outputs from the AWG to the oscilloscope.

waveforms using an arbitrary waveform generator (AWG) with a bandwidth of 500 MHz. A schematic of our experiment is shown in Fig. 1. We sample  $V(t)$  at a rate of 1.25 GHz, and input the sampled and normalized voltage sequence  $V[n]$  to Channel 1 of an AWG, which performs sinc-interpolation on the sample sequence supplied. At the same time, we input an ‘‘impulse’’ sequence  $I[n]$  (a sample of value 1, followed by an array of value 0) to Channel 2 of the AWG for triggering purposes. The AWG outputs  $V(t)$  and  $I(t)$ , the reconstructed continuous time signals from the sinc-interpolation process, to an oscilloscope through RF coaxial cables. Using  $I(t)$  as a trigger, we observe the reconstructed superoscillatory waveform with an enhanced sampling rate of 8 GHz to clearly resolve the superoscillatory features produced.

#### B. Generating Rapid Oscillations

First we demonstrate the generation of oscillations surpassing the high-frequency band limit. We construct a waveform with five cycles of superoscillations at 650 MHz—1.3 times the waveform bandwidth of 500 MHz. We choose to implement this waveform with 31 spectral components, giving us the freedom of placing 30 zeros on the  $z$ -plane. Following the design formulation in Section II-B, we close-pack 11 zeros on the unit circle, at an angular separation

$$\Delta\phi' = \frac{2\pi}{(N-1)R} = \frac{2\pi}{30 \times 1.3} \text{ rad.} \quad (12)$$

We then place the remaining 19 zeros in the sideband region to minimize the peak sideband amplitude [21], thus improving waveform sensitivity. Fig. 2(a) and (b) shows the resultant zero locations from our waveform design algorithm, and the corresponding frequency spectrum of the waveform. Fig. 2(c) shows excellent agreement between the calculated and experimentally observed temporal waveforms. Slight deviations are likely caused by the filtering effects of the electronic system. Fig. 2(d) shows a close up on the region of superoscillation, again showing excellent calculation-experiment agreement in this fast oscillation region. A 650-MHz sinusoid is nicely fitted onto the superoscillation ripples to show that superoscillation at 1.3 times the bandwidth limit is indeed achieved. To the best of our knowledge, this is the first experimental construction of a superoscillatory wave in the time domain.

#### C. Superoscillatory Pulse Compression

Having demonstrated the generation of rapid oscillations beyond a waveform’s bandwidth limit, we now proceed to con-

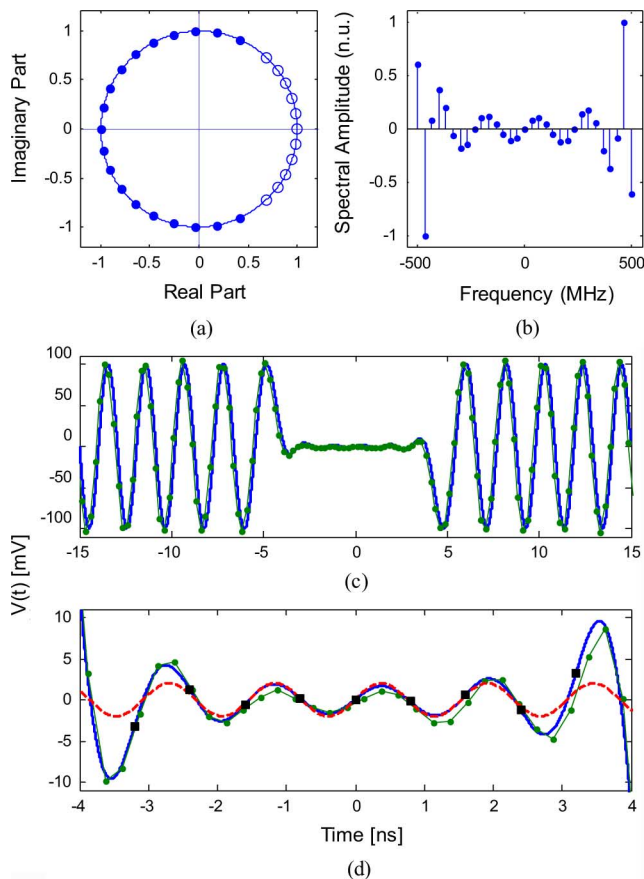


Fig. 2. Experimental demonstration of temporal superoscillation. (a) Zero locations for a waveform with five cycles of superoscillations at 650 MHz, which is 1.3 times the pulse bandwidth limit of 500 MHz. Empty circles denote zeros in the superoscillatory design region, while filled circles denote those outside the superoscillatory design region. (b) Corresponding spectral amplitudes (normalized). (c) Temporal profile of a period of the waveform, showing good agreement between calculation (blue in online version) and experimental observation (green in online version, dotted). (d) Close-up on the superoscillatory design region, comparing the experimental observation (green in online version, dotted) against calculation (blue in online version), and shows excellent agreement between the two. Comparison with a 650-MHz sinusoid (red in online version, dashed) indicates that superoscillation at 1.3 times the bandwidth limit is indeed achieved. Black squares denote sample points supplied to the AWG.

struct a superoscillatory pulse that is temporally compressed beyond the Fourier transform limit. We use 27 spectral lines evenly spread between  $\pm 500$  MHz, which gives us freedom to locate 26 zeros on the  $z$ -plane. We locate six zeros within the superoscillatory design interval  $T_d = 3$  ns using the polynomial expansion method outlined in Section II-C. With this expansion, we construct a waveform with the narrowest possible pulsewidth and sidelobe levels below 20% of the peak amplitude. As in the previous example, we place the remaining 20 zeros outside the superoscillatory region to minimize the sideband amplitude [21]. Fig. 3(a) and (b) shows the resulting zero locations and the corresponding spectral amplitude. Fig. 3(c) shows a period of the temporal waveform. Fig. 3(d) shows a close-up across the design interval. Once again the calculated and experimental temporal profiles align with excellent agreement. The pulsewidths at full width at half maximum (FWHM) are 0.78 ns (calculation) and 0.82 ns (experiment), which are 55% and 47%, respectively, improved beyond a transform-limited sinc waveform, for which

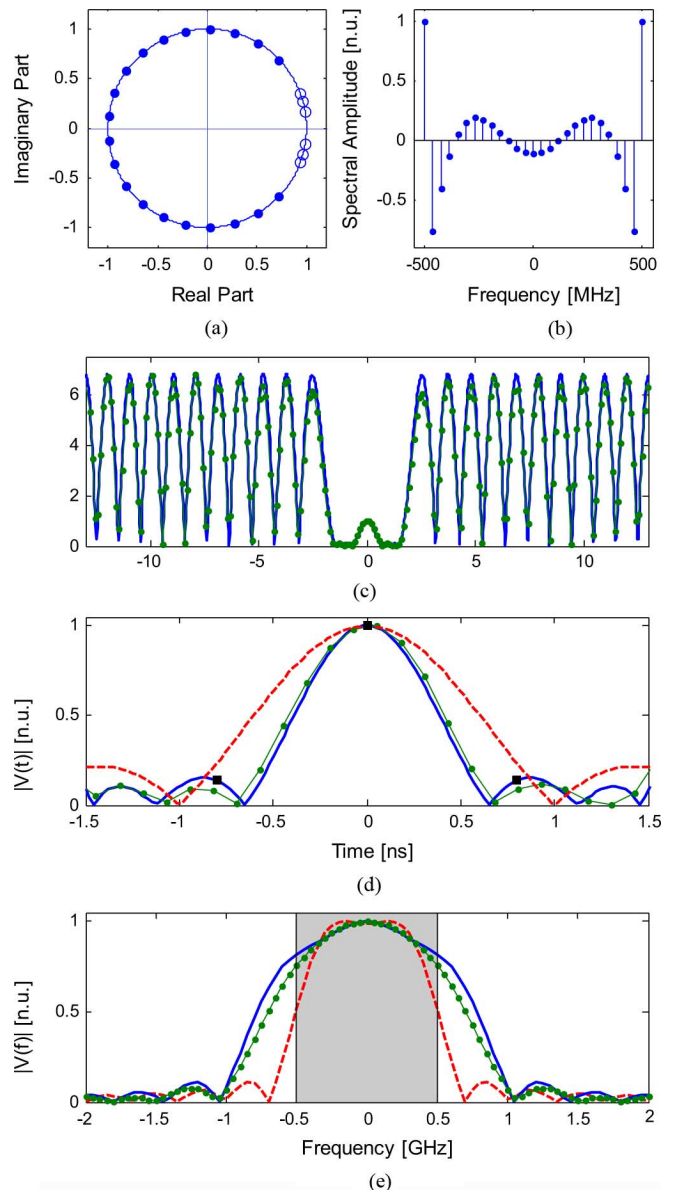


Fig. 3. Temporal pulse compression beyond the transform limit. (a) Zero locations for a temporally compressed superoscillation pulse. Empty circles denote zeros in the superoscillatory design region, while filled circles denote those outside the superoscillatory design region. (b) Corresponding spectral amplitudes (normalized). (c) Temporal profile of a period of the waveform, showing good agreement between calculation (blue in online version) and experimental observation (green in online version, dotted). Sideband amplitudes are 6.8 times the pulse peak amplitude. (d) Close-up on the superoscillatory design region, comparing the experimental observation (green in online version, dotted), against calculation (blue in online version) and a transform-limited sinc pulse (red in online version, dashed). Their respective voltage FWHMs are 0.82 ns (experiment), 0.78 ns (calculated), and 1.21 ns (sinc pulse). Black squares denote sample points supplied to the AWG. (e) Spectrum of the waveforms as truncated at the superoscillatory design region, again comparing experiment, calculation and the transform-limited sinc (same labeling as above). The superoscillatory waveform has considerable spectral component in the region (shaded) beyond that obtained from truncating the diffraction-limited sinc function. This explains the observation of variations faster than 500 MHz within this temporal region.

the FWHM measures 1.21 ns. This pulsewidth can be further improved through tradeoffs with the duration of the design interval and the sideband amplitude.

Fig. 3(e) shows the spectrum of the waveform if it were truncated to include only the superoscillatory region. We see

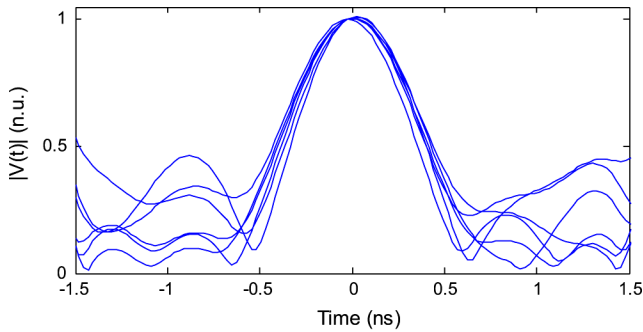


Fig. 4. Sensitivity analysis of the superoscillation waveform. The plot shows typical wave profiles across the superoscillation region when all spectral components of the waveform are subject to a randomly phased white Gaussian noise with amplitude 1.5% of the strongest spectral component. While sidelobes levels increase, the pulse shape and pulsewidth remains intact amidst this noise level.

that both the calculated and experimental spectra are decidedly wider than the spectrum of a sinc function truncated across the same interval. From this we can conclude that the effective bandwidth for a superoscillatory waveform is indeed widened in the time interval of superoscillation. We shall later elaborate on the potential of using a truncated superoscillatory filter as a simple way to expand the bandwidth of a pulse.

#### IV. DISCUSSION

The main result of this paper is the experimental demonstration of time-domain superoscillation, and the realization of pulse compression beyond the Fourier transform limit. However, in the following, we elaborate on a few implications of our foregoing formulation and experimentation.

##### A. Sensitivity Analysis

We first investigate the tolerable sensitivity of the generated pulse from a theoretical perspective. We model the precision of the generated spectral weights with a randomly phased white Gaussian noise with mean amplitude 1.5% of the strongest spectral component. Fig. 4 shows typical pulse magnitude variations when this spectral noise is added to our waveform. Amidst this small level of noise, we observe the emergence of stronger and asymmetric sidelobes within the design region, but the sub-transform limited pulsewidth is preserved. Thus, we see that our designed waveform achieves a level of reasonable robustness required for practical waveform generation.

We now examine the transmission characteristics of our experimental system for which the frequency response is given in Fig. 5. The frequency response is obtained by applying a Fourier transform to an “impulse” sequence. As shown, the spectral phase response is mostly linear across the range  $|f| \leq 500$  MHz. The spectral amplitude, however, contains a spike around dc, and slight modulations across this stretch. In our experiments, we compensated the system’s dc offset by introducing an opposing dc offset to our sample sequence before inputting it to the AWG. However, we were able to observe the designed superoscillatory signal without correcting for the slight spectral amplitude modulations. The fact that our designed superoscillatory waveforms tolerate these slight modulations shows their robustness and practicality—which is

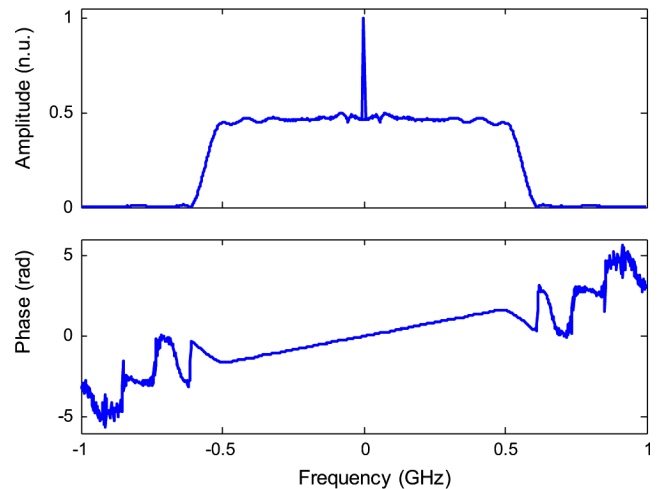


Fig. 5. Frequency response of the experimental system, consisting of the AWG, DSO, and connecting cables.

a primary objective of our design methodology. Pre-compensation—adjusting the input through dividing the source spectrum by the system’s transfer function—might be necessary when one wishes to construct superoscillatory waveforms with higher sensitivity.

##### B. Fast Varying Signal Synthesis

From Figs. 2(d) and 3(d), we observe that sample points sent to the AWG are sparse in the superoscillatory region relative to variations of the waveform. From a conventional perspective on the Nyquist limit, these sample points, which are spaced more than half an oscillation cycle apart, appear inadequate at capturing the rapid variations within the waveforms. However, the variations are faithfully restored upon the low-pass filtering digital-to-analog conversion process, due to the superoscillatory nature of the waveform. This demonstrated capability of generating fast varying temporal waveforms beyond the Nyquist limit (hence, also the Fourier transform limit) enables the generation of short pulses and other waveforms, which are traditionally deemed impossible for a specific bandwidth. There are, of course, two caveats to this scheme. Firstly, high-energy sidebands accompany the superoscillatory waveform. Secondly, the strength of the superoscillation forms a tradeoff with waveform sensitivity—as required by the Shannon limit [22]. Notwithstanding, in the preceding we have demonstrated the realization of superoscillatory sharp pulses with reasonable sensitivity. Thus, this scheme should see potential application in situations where one desires the fastest varying waveform from a system with stringent band limitation.

##### C. Bandwidth Extension

A further extension to synthesizing superoscillatory fast varying signals is to truncate the sidebands altogether. Fig. 3(e) shows the spectra of the calculated and experimental waveforms, after they are truncated to include only the superoscillatory region. While temporal truncation itself can be seen as a nonlinear, and hence, bandwidth extension process, from Fig. 3(e) we observe that truncating a superoscillatory signal

expands the signal bandwidth much more dramatically. Hence, we see that superoscillatory waveform generation, followed by a sideband-discarding truncation, form a simple bandwidth extension tool potentially useful for ultra-wideband wireless communication or spectroscopic applications that require wide bandwidth signals. Admittedly much waveform power will be discarded in a simple truncation process. Nonetheless, the corresponding bandwidth extension can be of great use in aforementioned applications, where power amplification is available, and where one can afford to tradeoff power efficiency for a gain in effective bandwidth. On the other hand, it would be a valuable direction of research to investigate whether parts of the truncated power from the sidebands can be reintegrated back into the system, perhaps through a feedback mechanism.

## V. CONCLUSION

In this paper, we have experimentally demonstrated temporal pulse compression beyond the Fourier transform limit. We adapted methods of superdirective antenna design to synthesize sub-transform limit waveforms in a well controlled manner. Our first realization of a temporal pulse 47% compressed beyond the Fourier transform limit, besides being an endeavour of scientific interest, should also prove applicable to realms such as time-domain measurement and synchronization, probing ultrafast dynamics, and object range detection.

## APPENDIX

*Surpassing the Fourier Transform Limit:* The Fourier Transform limit can be stated as an inequality stating a definite lower bound on the temporal and spectral width of a waveform [1], [23]

$$\Delta\omega\Delta t \geq C \quad (13)$$

where the constant  $C$  is on the order of  $2\pi$ , but its exact value depends on the waveform characteristics and the way in which the temporal and spectral widths are measured. In the microwave community where one has to contain an entire waveform within a specified bandwidth, temporal widths are often compared to those of a sinc distribution which makes “full use” of the available bandwidth. In this context, and measuring the temporal width at the voltage full-width-half-maximum, the temporal width limit becomes

$$\Delta t \geq \frac{3.789}{\Delta\omega} \quad (14)$$

where  $\Delta\omega$  is the spectral width over which the waveform is nonzero.

With temporal superoscillations, while the overall spectral width remains the same, a local spectral width is widened over a predefined time interval. As a result,  $\Delta t$  of the waveform, over that predefined interval, can be compressed beyond the lower bound stated in (14). Figs. 3(a)–3(d) shows such a temporal pulse, which we have designed and experimentally realized. The large amplitude sidebands are an inevitable artifact which

accompanies temporal superoscillations [19]. However, while those sidebands widen the total temporal width of the waveform, one can design the waveform such that the sidebands are sufficiently separated from the interval where superoscillatory features appear. In this manner, through superoscillation one can locally compress a temporal waveform beyond the Fourier Transform limit.

## REFERENCES

- [1] G. B. Folland and A. Sitaram, “The uncertainty principle: A mathematical survey,” *J. Fourier Anal. Appl.*, vol. 3, pp. 207–238, May 1997.
- [2] I. Arnedo, M. A. G. Laso, F. Falcone, D. Benito, and T. Lopetegui, “A series solution for the single-mode synthesis problem based on the coupled-mode theory,” *IEEE Trans. Microw. Theory Tech.*, vol. 56, no. 2, pp. 457–466, Feb. 2008.
- [3] I. Arnedo, J. D. Schwartz, M. A. G. Laso, T. Lopetegui, D. V. Plant, and J. Azana, “Passive microwave planar circuits for arbitrary UWB pulse shaping,” *IEEE Microw. Wireless Compon. Lett.*, vol. 18, no. 7, pp. 452–454, Jul. 2008.
- [4] A. Baltuska, Z. Wei, M. S. Pshenichnikov, and D. A. Wiersma, “Optical pulse compression to 5 fs at a 1-MHz repetition rate,” *Opt. Lett.*, vol. 22, pp. 102–104, Jan. 1997.
- [5] M. Nisoli, S. D. Silvestri, and O. Svelto, “Compression of high-energy laser pulses below 5 fs,” *Opt. Lett.*, vol. 22, pp. 522–524, Apr. 1997.
- [6] D. T. Reid, “Few cycle EM pulses,” *Contemp. Phys.*, vol. 40, pp. 293–204, May 1999.
- [7] Y. Aharonov, J. Anandan, S. Popescu, and L. Vaidman, “Superpositions of time evolutions of a quantum system and a quantum time-translation machine,” *Phys. Rev. Lett.*, vol. 64, pp. 2965–2968, Jun. 1990.
- [8] M. V. Berry, “Faster than Fourier,” in *Quantum Coherence and Reality: In Celebration of the 60th Birthday of Yakir Aharonov*, J. S. Anan and J. L. Safko, Eds. Singapore: World Sci., 1994, pp. 55–65.
- [9] M. V. Berry, “Evanescent and real waves in quantum billiards and Gaussian beams,” *J. Phys. A, Math. Gen.*, vol. 27, pp. L391–L398, Jun. 1994.
- [10] P. J. S. G. Ferreira, A. Kempf, and M. J. C. S. Reis, “Construction of Aharonov–Berry’s superoscillations,” *J. Phys. A, Math. Gen.*, vol. 40, pp. 5141–5147, May 2007.
- [11] F. M. Huang and N. I. Zheludev, “Super-resolution without evanescent waves,” *Nano Lett.*, vol. 9, pp. 1249–1254, Jan. 2009.
- [12] A. M. H. Wong and G. V. Eleftheriades, “Adaptation of Schelkunoff’s superdirective antenna theory for the realization of superoscillatory antenna arrays,” *IEEE Antennas Wireless Propag. Lett.*, vol. 9, pp. 315–318, Apr. 2010.
- [13] D. Schlichthärle, *Digital Filters: Basics and Design*. Berlin, Germany: Springer-Verlag, 2000.
- [14] S. A. Schelkunoff, “A mathematical theory of linear arrays,” *Bell Syst. Tech. J.*, vol. 22, pp. 80–107, Jan. 1943.
- [15] H. J. Riblet and C. L. Dolph, “A current distribution for broadside arrays which optimizes the relationship between beam width and side-lobe level,” *Proc. IRE*, vol. 35, no. 5, pp. 489–492, May 1947.
- [16] N. Yaru, “A note on super-gain antenna arrays,” *Proc. IRE*, vol. 39, no. 9, pp. 1081–1085, Sep. 1951.
- [17] M. Abramowitz and I. A. Stegun, *Handbook of Mathematical Functions: With Formulas, Graphs, and Mathematical Tables*. New York: Dover, 1972.
- [18] N. I. Zheludev, “What diffraction limit?,” *Nat. Mater.*, vol. 7, pp. 420–422, Jun. 2008.
- [19] P. J. S. G. Ferreira and A. Kempf, “Superoscillations: Faster than the Nyquist rate,” *IEEE Trans. Signal Process.*, vol. 54, no. 10, pp. 3732–3740, Oct. 2006.
- [20] R. C. Hansen, “Fundamental limitations in antennas,” *Proc. IEEE*, vol. 69, no. 2, pp. 170–182, Feb. 1981.
- [21] H. J. Orchard, R. S. Elliott, and G. J. Stern, “Optimising the synthesis of shaped beam antenna patterns,” *Proc. Inst. Elect. Eng.—Microw., Antennas, Propag.*, vol. 132, no. H, pp. 63–68, Feb. 1985.
- [22] A. Kempf, “Black holes, bandwidth and Beethoven,” *J. Math. Phys.*, vol. 41, pp. 2360–2374, Apr. 2000.
- [23] R. Paschotta, *Encyclopedia of Laser Physics and Technology*. Berlin, Germany: Wiley-VCH, 2008.



**Alex M. H. Wong** received the B.A.Sc. degree in engineering science and M.A.Sc. degree in electrical engineering from the University of Toronto, Toronto, ON, Canada, in 2006 and 2009, respectively, and is currently working toward the Ph.D degree at the University of Toronto.

His research interests include high-resolution imaging using electromagnetic waves, sub-wave-length focusing devices, metascreens, and super-oscillations.



**George V. Eleftheriades** (F'06) received the Diploma in Electrical Engineering degree from the National Technical University of Athens, Athens, Greece, in 1988, and the M.S.E.E. and Ph.D. degrees in electrical engineering from The University of Michigan at Ann Arbor, in 1989 and 1993, respectively.

From 1994 to 1997, he was with the Swiss Federal Institute of Technology, Lausanne, Switzerland. He is currently a Professor with the Department of Electrical and Computer Engineering, University of

Toronto, Toronto, ON, Canada, where he holds the Canada Research Chair/Velma M. Rogers Graham Chair in Engineering.

Prof. Eleftheriades was elected a Fellow of the Royal Society of Canada in 2009. He was an IEEE Antennas and Propagation Society (IEEE AP-S) Distinguished Lecturer (2004–2009) and a member of the IEEE AP-S Administrative Committee (AdCom) (2008–2010). He is a member of the Technical Coordination Committee MTT-15 (Microwave Field Theory). He is an associate editor for the IEEE TRANSACTIONS ON ANTENNAS AND PROPAGATION. He has been the general chair of the 2010 IEEE International Symposium on Antennas and Propagation and CNC/USNC/URSI Radio Science Meeting, Toronto, Japan. He was the recipient of the 2008 IEEE Kiyo Tomiyasu Technical Field Award, the 2001 Ontario Premiers' Research Excellence Award, the 2001 Gordon Slemmon Award presented by the University of Toronto, and the 2004 E. W. R. Steacie Fellowship presented by the Natural Sciences and Engineering Research Council of Canada (NSERC). He was the corecipient of the inaugural 2009 IEEE MICROWAVE AND WIRELESS COMPONENTS LETTERS' Best Paper Award and the 2008 RWP King Best Paper Award.